Resonant modes of dipole-coupled lattices

K. Rivkin,[1] A. Heifetz,[2] P. R. Sievert,[1] and J. B. Ketterson[1,2]
[1]*Department of Physics and Astronomy, Northwestern University, 2145 Sheridan Avenue, Evanston, Illinois 60208, USA*
[2]*Department of Electrical and Computer Engineering, Northwestern University, 2145 Sheridan Avenue, Evanston, Illinois 60208, USA*
(Received 13 January 2004; revised manuscript received 18 May 2004; published 8 November 2004)

A general method is developed to find the equilibrium magnetization and the eigenfrequencies (resonant modes) associated with a magnetic body of arbitrary shape based on the discrete dipole approximation. In this first of a series of papers the method is applied to the simple case of a line of dipoles with the magnetic field both parallel and perpendicular to the axis of the line.

DOI: 10.1103/PhysRevB.70.184410 PACS number(s): 76.50.+g, 75.10.Hk, 41.20.Gz

I. INTRODUCTION

Studying the response to a microwave magnetic field $\mathbf{H}_1$ in the presence of a strong static magnetic field $\mathbf{H}_0$ (e.g. ferromagnetic resonance or FMR) is a powerful technique to investigate the coherent dynamics of magnetic particles. Such experiments are typically carried out at frequencies on the order of 10^{10} Hz. Domain switching in inhomogeneously magnetized bodies occurs at comparable rates.

Information about the exchange interaction, magnetic anisotropy, and dissipation processes in bulk ferromagnets can be obtained from the FMR technique. Size and shape play a role in modifying the resonance modes of nanoscale ferromagnetic particles. The collective behavior of the magnetization also involves coupling of the precessing uniform magnetization to the spin wave modes,[1] particularly at high rf drive levels. A detailed knowledge of how these phenomena affect the modes may ultimately be of practical interest since dynamical switching studies may offer a faster writing technology, while resonance probes may provide an alternative read technology.

Experiments on ferromagnetic resonance in ferrites have shown that under suitable conditions the power absorption at a fixed frequency may pass through a number of maxima as the dc magnetic field is varied. A necessary condition for the excitation of these features is that the rf magnetic field at the sample be inhomogeneous. In experiments involving insulating ellipsoidal ferrites the rf exciting fields are not expected to change rapidly over a small sample and the wavelengths of the excited modes are generally comparable with the dimensions of the body. If exchange is neglected, these modes can be calculated, to a very good approximation, by using a magnetostatic condition, $\nabla \times \mathbf{H} = 0$, and hence they are called magnetostatic modes. Mercereau and Feynman[2] identified a few of the more simple distributions for a sphere, and Walker[3,4] calculated all the possible solutions for a spheroid. The resulting modes were numbered by the indices of associated Legendre polynomials and a periodic exponential function. Fletcher and Bell[5,6] and Plumier[7] carried out an extensive analysis and numerical calculations for spheres, providing tables for various solutions. The physical nature of the magneto-static modes was later partially clarified by the work of Damon and Eshbach.[8]

Walker's analysis was formulated in terms of a continuum-matter, magnetostatic boundary-value problem. In this paper, we explore a numerical approach based on a model involving N discrete dipoles, often called the *discrete dipole approximation*. One can also trivially add exchange effects, which is not the case with the analytic approaches. The first attempt to use a discrete dipole approach for magnetostatic spin waves was done by Politi *et al.*[9] A disadvantage of the discrete dipole approach is that, since it reduces to an eigenvalue problem for which the size of the associated matrix is $2N \times 2N$, the eigenvalue routines ultimately down break for large numbers of particles.

Our approach involves a solution of the coupled Larmor equations of the individual dipoles with all fields acting on them explicitly accounted for (dipole, exchange, and magnetic anisotropy). It can be viewed as a discrete version of the Landau-Lifshitz equation. For small oscillation amplitudes we can recast the problem as a system of linear equations, where the eigen-frequencies are the resonant modes, and the eigenvectors are the relative amplitudes of excitation of the individual dipoles.

A natural question is how the modes of our discrete dipole model relate to those of Walker. The case of simple cubic packing within a sphere with a given radius roughly corresponds to the results obtained by Walker and Fletcher for a continuum sphere. An unavoidable problem that arises in trying to make such a comparison is that the cubic packing will always be restricted to the symmetries of a cube, while the analytic continuum solution of Walker has the full symmetry of the sphere. We have not as yet been able to devise a method to unambiguously associate our eigenfrequencies with those of the continuum model. It would be of interest to pursue this problem.

An advantage of our approach lies in the fact that we can apply the method to particles of arbitrary shape, for which analytical solutions cannot be constructed. This is particularly relevant for cylindrical- and disk-shaped nanoparticles, which are relatively easy to pattern experimentally and are of much current interest. In recent years a few articles have been published that discuss the dynamic properties of discrete dipole structures.[10] There is also significant interest in studying the equilibrium configurations of magnetic structures; however these works are not explicitly related to the present study.

Recently a technique was proposed to "scale" static discrete dipole calculations for smaller size objects to describe larger systems.[11] Extending this to scale the dynamical properties discussed here would be of great interest.

II. MICROMAGNETICS STRATEGIES

Here we present our strategy to model the magnetic properties of magnetic nanostructures.

Only ellipsoids and degenerate forms thereof can have a uniform magnetization. All other shapes are nonuniformly magnetized. The exchange interaction prefers to keep the magnetization of all spins parallel, but dipolar shape effects compete to make this direction position dependent in a nonellipsoidal body. One usually assumes that the *magnitude* of the magnetization is constant and we will assume this, although this may not be the case for small (near-superparamagnetic) particles or near the transition temperature. Our model is based on simply summing the magnetic field from discrete, point dipoles that uniformly fill the body in question on some grid.[11] The magnetic moment of these particles is fixed so as to reproduce the magnetization **M** (i.e., the magnetic moment per unit volume) of the body in question. Thus the field on a dipole i is given by summing over the fields produced by the remaining dipoles, j, which is given by the usual form

$$\mathbf{h}_i^{dipole} = \sum_{j\neq i} \mathbf{m}_j \left(\boldsymbol{\nabla}\,\boldsymbol{\nabla} \left(\frac{1}{r_{ij}} \right) \right) = \sum_{j\neq i} \left[\frac{3\mathbf{r}_{ij}(\mathbf{m}_j \cdot \mathbf{r}_{ij})}{r_{ij}^5} - \frac{\mathbf{m}_j}{r_{ij}^3} \right]. \tag{2.1}$$

To account for the exchange interaction we can add a second "effective" or "exchange" field on the ith dipole of the nearest-neighbor Heisenberg type:

$$\mathbf{h}_{\text{exchange}} = J \sum_{NN} \mathbf{m}. \tag{2.2}$$

The exchange constant J would be adjusted to reproduce the experimental continuum limit coefficient of the gradient energy.[12] Surface pinning will arise naturally since these moments have no neighbors; it could be adjusted by altering J for surface or-near surface moments. J in general needs to be scaled according to the prescription used to discretize the body.

The sum of the dipole, exchange and external field, $\mathbf{H}_0$, acting on the ith dipole is then given by

$$\begin{aligned} \mathbf{h}_i &= \mathbf{h}_i^{dipole} + \mathbf{h}_i^{exchange} + \mathbf{H}_0 \\ &= \sum_{j\neq i} \left[\frac{3\mathbf{r}_{ij}(\mathbf{m}_j \cdot \mathbf{r}_{ij})}{r_{ij}^5} - \frac{\mathbf{m}_j}{r_{ij}^3} \right] + \mathbf{h}_i^{exchange} + \mathbf{H}_0. \end{aligned} \tag{2.3}$$

The crystalline anisotropy energy for the uniaxial case has the form $E_A = K \sin^2 \theta$. The resultant torque, $N_A = \partial E_A / \partial \theta$, may be written in a vector form as

$$\mathbf{N}_A = K \frac{(\mathbf{m} \cdot \hat{\mathbf{H}}_A)\mathbf{m} \times \hat{\mathbf{H}}_A}{m^2},$$

$$H_A^{\text{eff}} = \frac{K(\mathbf{m} \cdot \hat{\mathbf{H}}_A)}{m^2} \hat{\mathbf{H}}_A = \frac{K(\mathbf{m} \cdot \hat{\mathbf{H}}_A)}{m^2} \hat{\mathbf{H}}_A, \tag{2.4}$$

where the unit vector $\hat{\mathbf{H}}_A$ points along the anisotropy axis; for an easy axis system K is positive while for the easy-plane system it is negative. In the examples treated in the article we will limit ourselves to dipole-dipole and exchange interactions only.

We have used four different methods to find the equilibrium configuration.

(1) One approach is to perform a Runge-Kutta integration of the Landau-Lifshitz equation with a damping term and a random starting configuration. This method has numerous disadvantages.

(a) For long running times, one needs to introduce tricks in order to keep the magnitude of dipole moment constant.

(b) Unstable configurations that have no torque acting on the dipoles, unless some perturbation is introduced, can be made stable by the presence of damping.

(c) In some cases the ground state and a few metastable states can coexist. In such a case the final configuration depends on the initial configuration of the integration. (This will be discussed in detail in Sec. IV E.)

(2) A second approach is the Monte-Carlo method. With enough samples a state very close to the true ground state can be located. However this approach becomes very slow for more than a few dipoles.

(3) In the third approach we choose the initial directions randomly and rotate the dipoles so as to maximize the gradient in the energy. By moving to these directions, evaluating the energy and again reorienting the dipoles so as to maximize the gradient, we may continue until the decrease in energy drops below some preset value. This method gave us mixed results—it worked well for some configurations, but in other cases it would become trapped in regions with very small energy gradients for too long. As can be shown, for certain unstable configurations some external intervention is required to force the system out of such traps.

(4) The most successful approach involved a relaxation-like method. Here we start with a random configuration of spins. We then calculate the field at position i arising from Eq. (2.3). Then we align each magnetic moment parallel to the new local field. We continue this process of inserting the moments into (2.3) and reorienting them until the local fields stabilize. This can be taken as the initial (equilibrium) magnetic configuration of the particles.

With this method one can occasionally become trapped by repetitively jumping between two unstable configurations, but for most situations it proved to be the fastest and most reliable. Unstable configurations with no torque acting on the dipoles are highly improbable, and even small deviations force the system to walk away from them.

As with the Runge-Kutta integrations, in the presence of metastable states, the final configuration depends on the initial, randomly chosen, starting point. However we are free to quickly try new starting configurations.

III. FERROMAGNETIC RESONANCE

The resonant modes follow from the solution to the Larmor equation,

$$\frac{d\mathbf{m}_i}{dt} = -\gamma \mathbf{m}_i \times \mathbf{h}_i^{total}. \tag{3.1}$$

We linearize the problem by writing

$$\mathbf{m}_i = \mathbf{m}_i^{(0)} + \mathbf{m}_i^{(1)} \tag{3.2a}$$

and

$$\mathbf{h}_i^{total} = \mathbf{h}_i^{(0)} + \mathbf{h}_i^{(1)}. \tag{3.2b}$$

Inserting these expressions into Eq. (3.1) gives

$$\frac{d\mathbf{m}_i^{(1)}}{dt} = -\gamma[\mathbf{m}_i^{(0)} \times \mathbf{h}_i^{(1)} + \mathbf{m}_i^{(1)} \times \mathbf{h}_i^{(0)}], \tag{3.3}$$

where

$$\mathbf{h}_i^{(0)} = \mathbf{h}_i^{dipole} + \mathbf{h}_i^{exchange} + \mathbf{H}_0 = \sum_{j\neq i} \mathbf{m}_j^{(0)} \left(\nabla\,\nabla \left(\frac{1}{r_{ij}} \right) \right) + \mathbf{h}_i^{exchange} + \mathbf{H}_0 \tag{3.4a}$$

and

$$\mathbf{h}_i^{(1)} = \mathbf{h}_i^{dipole} + \mathbf{h}_i^{exchange} = \sum_{j\neq i} \mathbf{m}_j^{(1)} \left(\nabla\,\nabla \left(\frac{1}{r_{ij}} \right) \right) + \mathbf{h}_i^{exchange}. \tag{3.4b}$$

We assume a solution of the form

$$\mathbf{m}_i^{(1)}(t) = \mathbf{m}_i^{(1)} e^{-i\omega t}, \tag{3.5}$$

and Eq. (3.3) becomes

$$i\omega \mathbf{m}_i^{(1)} = \gamma[\mathbf{m}_i^{(0)} \times \mathbf{h}_i^{(1)} + \mathbf{m}_i^{(1)} \times \mathbf{h}_i^{(0)}]. \tag{3.6}$$

Using Eq. (3.4b) we can write Eq. (3.6) as

$$i\omega \mathbf{m}_i^{(1)} = \gamma \mathbf{m}_i^{(0)} \times \left[\sum_{j\neq i} \left[\frac{3\mathbf{r}_{ij}(\mathbf{m}_j^{(1)} \cdot \mathbf{r}_{ij})}{r_{ij}^5} - \frac{\mathbf{m}_j^{(1)}}{r_{ij}^3} \right] + \mathbf{h}_i^{exchange} \right] + \gamma \mathbf{m}_i^{(1)} \times \mathbf{h}_i^{(0)}. \tag{3.7}$$

Equation (3.7) has the structure of a vector eigenvalue problem. The solutions should contain all the (generally mixed) dipolar and spin-wave modes. By setting $J=0$ we can eliminate the exchange-coupled spin wave modes. To solve Eq. (3.7), one needs to rewrite the vector equation as a system of three coupled scalar equations (the *x*-, *y*-, and *z*-component projections of the vector equation).

Since in our problem the magnitude of unperturbed magnetic moment is a constant, we actually only have 2 independent components; hence by working with a set of coordinates aligned with the equilibrium direction of each dipole, one can rewrite Eq. (3.7) in a form involving only a $2N$ by $2N$ matrix. Although the appropriate equations were obtained, they were not implemented in the present study due to the increased complexity of coding the expressions involved. As a result one third of the eigenfrequencies returned using the three-component form of the equations will be zero.

An alternative to the eigenvalue approach is to directly integrate the Larmor equation for an assembly of spins using, say, the Runge-Kutta method. This is a powerful approach and routines that perform this integration are available.[13] A disadvantage is that it does not yield the eigenfrequencies directly, but only a large response to an external drive at specific frequencies.[14] One needs to perform the calculation for a range of frequencies and not all of the modes will be excited for a given drive field. One of the biggest advantages of the method presented in this paper is that it allows one to modify the original problem by assuming periodic boundary conditions in some of the directions, or by performing some sort of scaling, which allows one to work with millions of spins formed into a few thousand superspins. The practical implementation of such approaches will be discussed in future papers. However it should be emphasized that the Runge-Kutta method has the property that it is applicable to the nonlinear regime.

Suppose we have obtained a positive-frequency solution and the associated complex eigenvector:

$$\mathbf{m} = \mathbf{m}_{real} + i\mathbf{m}_{imag}. \tag{3.8a}$$

For the solution having the same magnitude of the frequency, but with the opposite sign, we have

$$\mathbf{m} = \mathbf{m}_{real} - i\mathbf{m}_{imag}, \tag{3.8b}$$

i.e., we have the complex conjugate eigenvector. So the true motion must be represented as

$$(\mathbf{m}_{real} + i\mathbf{m}_{imag})e^{-i\omega t} + (\mathbf{m}_{real} - i\mathbf{m}_{imag})e^{+i\omega t} = 2\mathbf{m}_{real}\cos\omega t + 2\mathbf{m}_{imag}\sin\omega t, \tag{3.9}$$

which is a real quantity.

IV. CALCULATIONS

For the sake of simplicity we will assume the particle number along each direction to be odd and given by (upper case) letters N_x, N_y and N_z where the total number of particles is then $N=N_xN_yN_z$; we identify the quantities $(N_{x,y,z}-1)/2$ with the (lower case) letters, n_x, n_y and n_z.

When we use periodic boundary conditions we "wrap" the sample around itself so that

$$\mathbf{m}_{N_{x,y,z}+q} = \mathbf{m}_q. \tag{4.1}$$

Assuming that the solutions of Eq. (3.7) are plane waves we have

$$\vec{m}_q = e^{i\vec{k}\cdot\vec{q}},$$

$$\vec{m}_{N_{x,y,z}+q} = \vec{m}_q; \quad e^{ik_{x,y,z}(N_{x,y,z}+q)} = e^{ik_{x,y,z}(q)} e^{2\pi p_{x,y,z}},$$

$$k_{x,y,z} = \frac{2\pi p_{x,y,z}}{N_{x,y,z}}, \tag{4.2}$$

$$\left(\frac{N_{x,y,z,}-1}{p_{x,y,z}} \right)_{min} = 2; \quad p_{max} = \frac{N_{x,y,z,}-1}{2} = n_{x,y,z};$$

$$p_{x,y,z} = -n_{x,y,z}, n_{x,y,z}-1, \ldots, 0, \ldots n_{x,y,z}.$$

Here $p_{x,y,z}$ are integers with values from $-n_{x,y,z}$ to $+n_{x,y,z}$. When these conditions apply the solutions are plane waves but because of the imposed boundary conditions they will have a discrete spectrum. Note the minimum possible wavelength in the sample is 2 (the lattice constant is equal to 1).

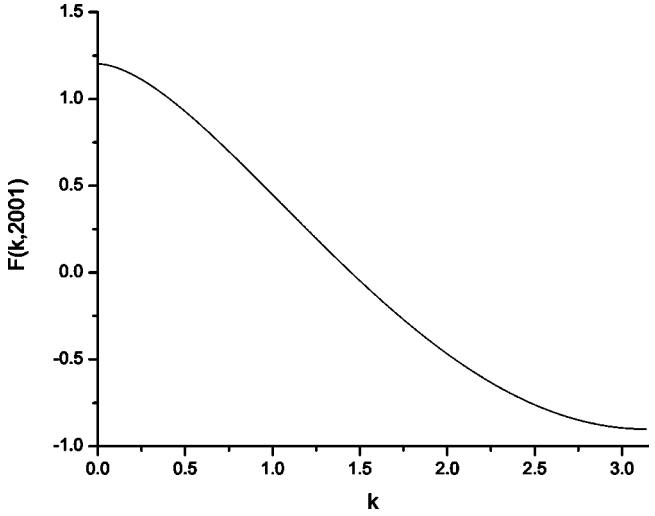

FIG. 1. $F(k,N)$ as a function of wavevector k; $N=2001$ dipoles.

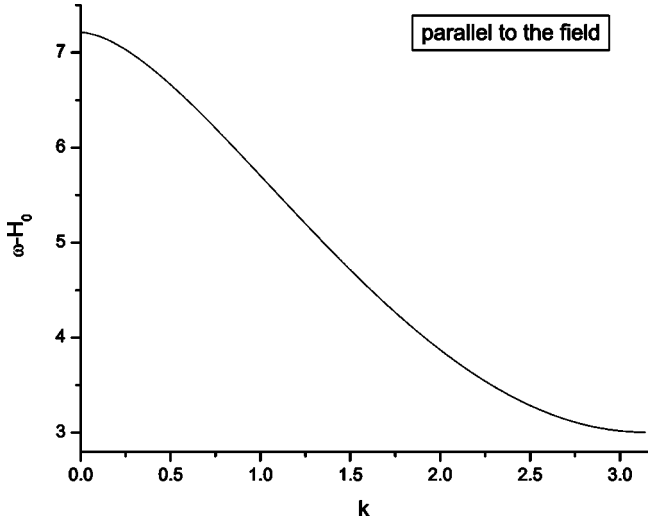

FIG. 2. Frequency as a function of wave vector with the sample parallel to the applied field; $n=1000$, $N=2001$ dipoles.

A. Bloch spin waves

We can apply this formalism to the case where we have an exchange interaction with an external magnetic field applied along the z direction, but no dipole-dipole interaction. In this case the local field is parallel to the external field and the solution for the case of periodic boundary conditions has the form

$$m_y^{(1)}(x,y) = +ie^{ik_x x}e^{ik_y y}e^{ik_z z};\ m_x^{(1)}(x,y) = e^{ik_x x}e^{ik_y y}e^{ik_z z};\ m_z = 0. \tag{4.3}$$

Using Eq. (3.7) and taking the x, y, and z coordinates to be discrete, and a lattice constant equal to 1, we have

$$\frac{\omega}{\gamma}e^{ik_x x}e^{ik_y y}e^{ik_z z} = M_s \sum_{r'\neq r,NN} (-Je^{ik_x x'+ik_y y'+ik_z z'}) + e^{ik_x x}e^{ik_y y}e^{ik_z z}\left(H_0 + M_s\sum_{NN} J\right),$$

$$-\frac{\omega}{\gamma}e^{ik_x x}e^{ik_y y}e^{ik_z z} = M_s \sum_{r'\neq r,NN} (Je^{ik_x x'+ik_y y'+ik_z z'}) - e^{ik_x x+ik_y y+ik_z z}\left(H_0 + M_s\sum_{NN} J\right), \tag{4.4}$$

where M_s is the saturation magnetization and H_0 is the external magnetic field; the sum is performed among nearest neighbors only. The resulting frequencies are then

$$\omega = \gamma H_0 + M_s\gamma J[6 - 2\cos(k_x) - 2\cos(k_y) - 2\cos(k_z)),$$

$$\omega \approx \gamma H_0 + \gamma J M_s k^2, \tag{4.5}$$

which is a well known formula for Bloch spin waves. The moments associated with these waves have a constant tipping angle but different relative phases. All modes, with the exception of one with $k_x=k_y=k_z=0$, have degeneracies—if we change the direction of propagation, we do not change the frequency of the wave.

B. Modes of a dipole-dipole coupled line parallel to an external field: Periodic boundary conditions

We will apply the above model to calculate magnetostatic resonance modes, or dipole spin waves, for the simple case of a line of atoms with the magnetic field both parallel and perpendicular to the line. We do this for the case of a line with free ends as well as one satisfying periodic boundary conditions.

We choose a coordinate system such that all the spins lie along the z-axis. The component of the eigenvectors parallel to the applied field vanishes, so that the oscillations are confined to the x-y plane. Equation (3.7) then takes the form

$$i\frac{\omega}{\gamma}m_{ix}^{(1)} = M_s\left(\sum_{j\neq i}\left(+\frac{m_{jy}^{(1)}}{r_{ij}^3}\right) + J(2m_{iy}^{(1)} - m_{(i-1)y}^{(1)} - m_{(i+1)y}^{(1)})\right) + m_{iy}^{(1)}\left(H_0 + \sum_{z=1..N_z}\left(\frac{4M_s}{|z|^3}\right)\right),$$

$$i\frac{\omega}{\gamma}m_{iy}^{(1)} = M_s\left(\sum_{j\neq i}\left(-\frac{m_{jx}^{(1)}}{r_{ij}^3}\right) - J(2m_{ix}^{(1)} - m_{(i-1)x}^{(1)} - m_{(i+1)x}^{(1)})\right) - m_{ix}^{(1)}\left(\frac{H_0}{M_s} + \sum_{z=1..N_z}\left(\frac{4M_s}{|z|^3}\right)\right). \tag{4.6}$$

If we assume a periodic boundary condition, we can solve these equations analytically in terms of the plane wave forms:

$$m_y^{(1)}(z) = e^{i\varphi}e^{ikz};\ m_x^{(1)}(z) = e^{ikz}. \tag{4.7}$$

From this we obtain

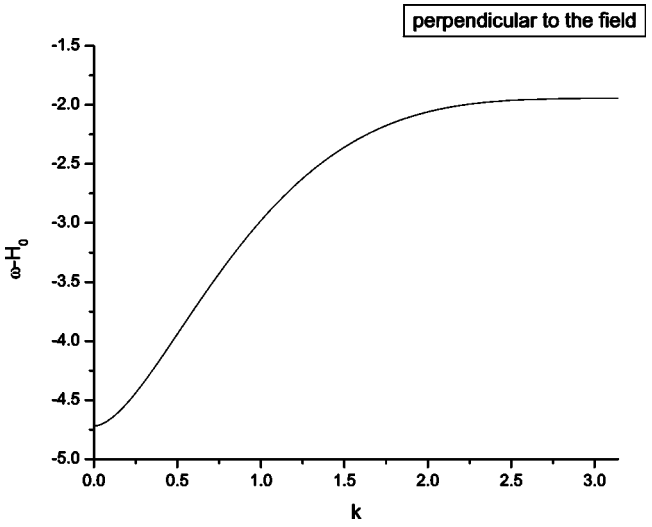

FIG. 3. Frequency as a function of the wave vector with the sample perpendicular to the applied field; $n=1000$, $N=2001$ dipoles, $H_0=10$.

$$e^{-2i\varphi} = -1; \quad \varphi = \frac{\pi}{2},$$

$$\omega = \gamma M_s \sum_{z' \neq z} \frac{e^{ik(z'-z)}}{r_{z'z}^3} + \gamma\left(H_0 + M_s \sum_{z' \neq z} \frac{2}{r_{z'z}^3}\right) + \gamma M_s J(2 - e^{-ik} - e^{ik}),$$

$$\sum_{z' \neq z} \frac{e^{ik(z'-z)}}{r_{z'z}^3} = 2\sum_{x'-x=1}^{N}\left(\frac{\cos(k(z'-z))}{(z'-z)^3}\right) = 2\sum_{d=1}^{N}\left(\frac{\cos(kd)}{d^3}\right) = 2F(k,N), \tag{4.8}$$

$$\sum_{d=1}^{N}\left(\frac{1}{d^3}\right) = F(0,N),$$

$$\omega = 2\gamma M_s F(k,N) + \gamma M_s 4F(0,N) + \gamma H_0 + 2\gamma M_s J(1-\cos(k)).$$

Figure 1 shows the behavior of the function $F(N,k)$ as a function of k.

Hereafter for the figures we will assume for simplicity, $\gamma=1$, $M_s=1$, $a=1$. The dispersion curve is given in Fig. 2 (positive k only).

C. Modes of a dipole-dipole coupled line perpendicular to an external field: Periodic boundary conditions

Here we only treat the case where the field is sufficiently high that in equilibrium the spins are essentially aligned along the applied magnetic field (this requires fields above ≈ 7.2 in our units), the low-field behavior will be discussed in Sec. IV E. Unlike the previous case, where the orbits were circular, here they are in general elliptical.

Similar to the previous case we obtain

$$i\frac{\omega}{\gamma}m_{ix}^{(1)} = M_s\sum_{j\neq i}\left(\frac{m_{jy}^{(1)}}{r_{ij}^3} - Jm_{jy}^{(1)}\right) + m_{iy}^{(1)}\left(H_0 + M_s\sum_{j\neq i}\left(-\frac{1}{r_{ij}^3} + J_{NN}\right)\right),$$

$$i\frac{\omega}{\gamma}m_{iy}^{(1)} = M_s\sum_{j\neq i}\left(\frac{3(x_i-x_j)^2 m_{jx}^{(1)}}{r_{ij}^5} - \frac{m_{jx}^{(1)}}{r_{ij}^3} + J_{NN}m_{jx}^{(1)}\right) - m_{ix}^{(1)}\left(H_0 + M_s\sum_{j\neq i}\left(-\frac{1}{r_{ij}^3} + J_{NN}\right)\right), \tag{4.9}$$

where J_{NN} appears only in the sum among nearest neighbors.

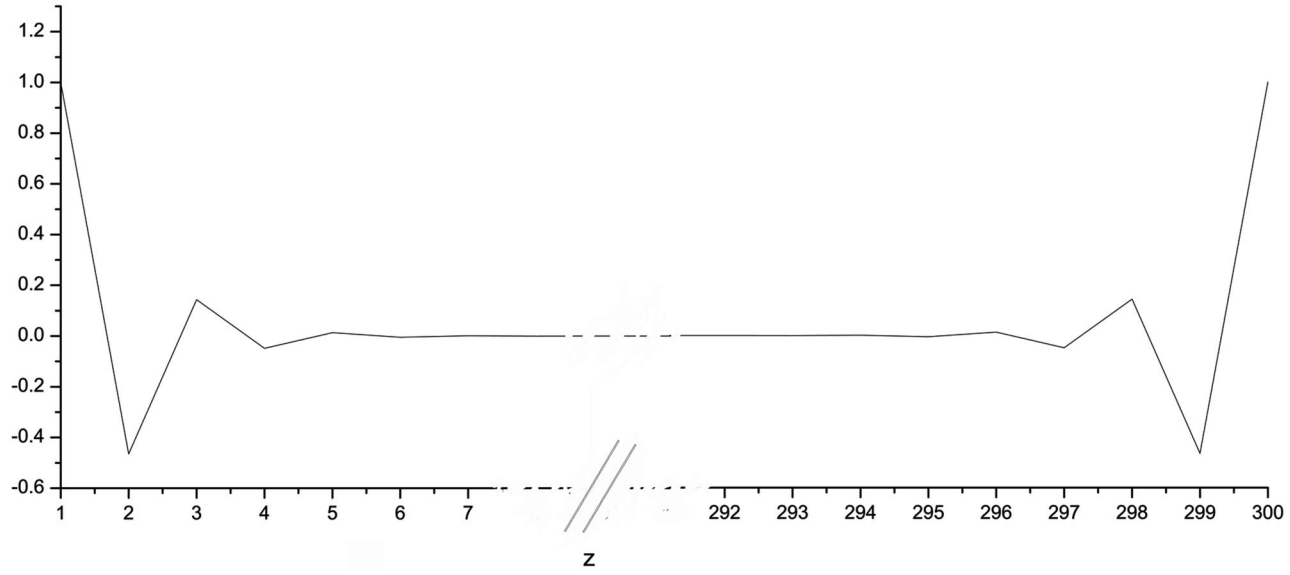

FIG. 4. Amplitude as a function of z for an "end" mode; 1500 dipoles.

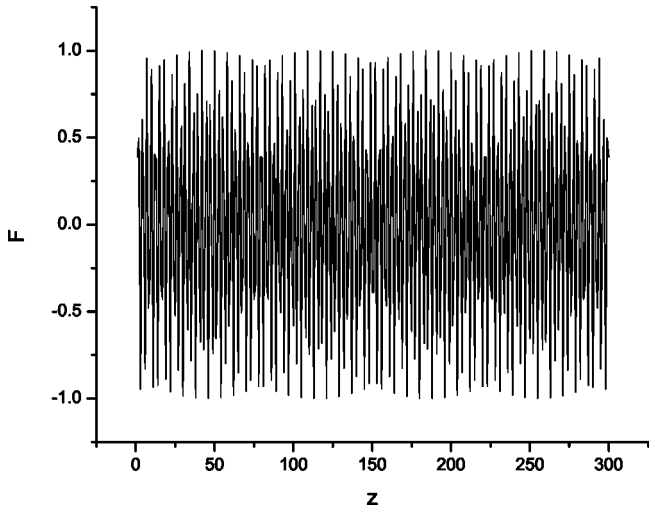

FIG. 5. Mode amplitude as a function of dipole coordinate z for the "bulk-pi" mode; $N=300$ dipoles.

We now seek solutions of the form

$$m_y^{(1)}(x) = be^{i\varphi}e^{ikx};\quad m_x^{(1)}(x) = ae^{ikx}; \tag{4.10}$$

in this case a^2/b^2 is a measure of the ellipticity of the orbits. Using the fact that $F(k,N)$ is always real, and from two possible values for $e^{i\varphi}$, we choose the one corresponding to positive frequencies.

The solution is

$$\varphi = \frac{\pi}{2};$$

$$\frac{a^2}{b^2} = 1 + \frac{6F(k,N)}{-4F(k,N) + 2J(1-\cos(k)) + \dfrac{H_0}{M_s} - 2F(0,N)},$$

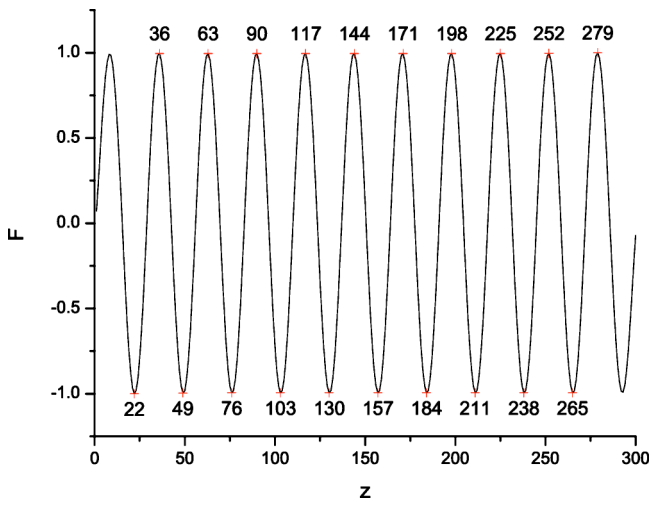

FIG. 6. Mode amplitude as a function of dipole coordinate z for the "bulk" mode; $N=300$ dipoles.

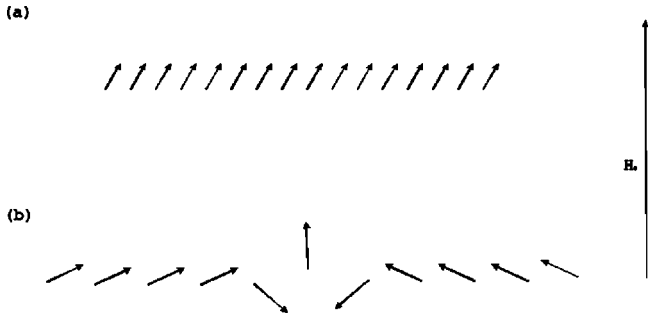

FIG. 7. Example of low-field equilibriums occurring in a line perpendicular to the external magnetic field. (a) Ground state; (b) "domain" state.

$$\omega^2 = \gamma^2 M_s^2\left[2F(k,N) + 2J(1-\cos(k)) + \frac{H_0}{M_s} - 2F(0,N)\right] \times\left[-4F(k,N) + 2J(1-\cos(k)) + \frac{H_0}{M_s} - 2F(0,N)\right] \tag{4.11}$$

where $F(k,N)$ was defined in the previous section.

At high fields a^2/b^2 approaches 1, approximately as $1/H_0$, implying that the orbits are circular in this limit.

Since $F(k,N)$ changes sign for $k=\pi/2$, a^2/b^2-1 also changes sign at this point and modes with smaller k have $a>b$, with the semi-major axis of oscillation aligned with the sample axis; modes with larger k have $a<b$, and have the semi-major axis of oscillation perpendicular to the sample axis. The dispersion relation is shown in Fig. 3. Again, all modes but the one with $k=0$ are degenerate for forward and backward traveling waves.

D. Modes for a dipole-dipole coupled line parallel to an external field: Nonperiodic boundary conditions

We start with Eq. (4.6), but this time there are no boundary conditions, i.e., no artificial "wrapping" of the line. In

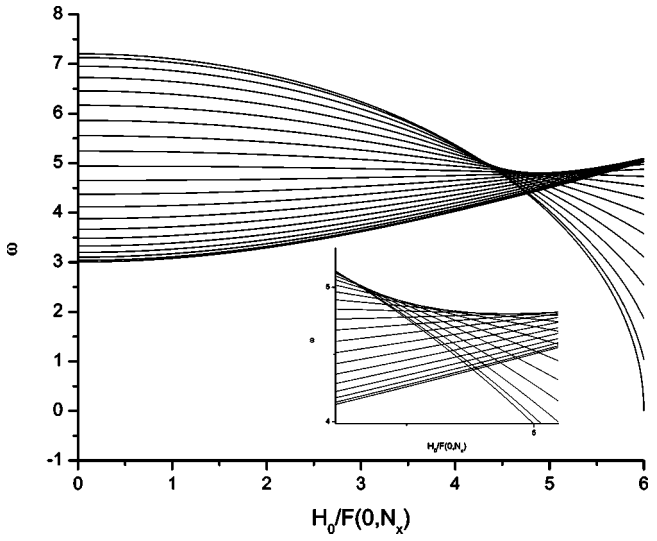

FIG. 8. Eigenfrequencies of a low-field ground state; $J=0$, 21 dipoles.

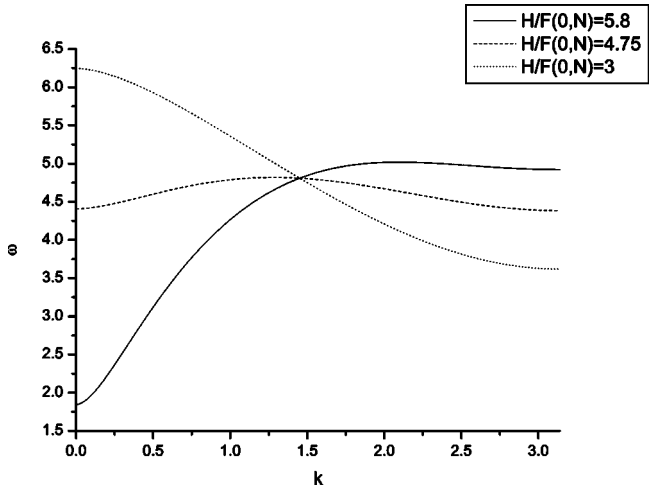

FIG. 9. Dispersion curves of a low-field ground state and different values of the applied field; $J=0$, 1001 dipoles.

this case the local magnetic field is a function of a coordinate z and we cannot obtain a simple solution in terms of plane waves; we must therefore find the eigenfrequencies numerically.

In this case the solution can be represented as

$$m_y^{(1)}(z) = iF(z),\ m_x^{(1)}(z) = F(z). \tag{4.12}$$

Solving for $F(z)$ numerically we find that there are three types of oscillations present in the system.

One of these we refer to as "pi-modes" which are characterized by a phase shift of π between neighboring dipoles. However there are two types of "pi-modes"—"end" symmetric and anti-symmetric modes that exist only close to the ends of the line (Fig. 4—this type of oscillation was first reported by Politi *et al.*[9]), and which exponentially decrease inside the sample. We also find "bulk pi modes" which are characterized by a periodic envelope (Fig. 5).

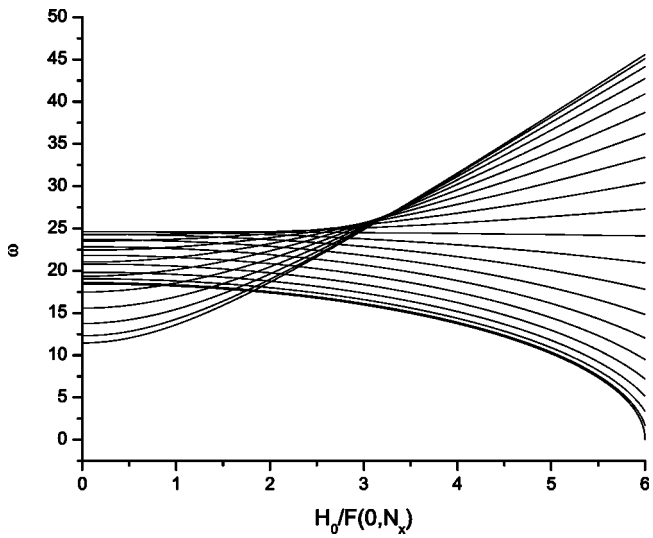

FIG. 10. Eigenfrequencies of a low-field ground state; $J=10$, 21 dipoles.

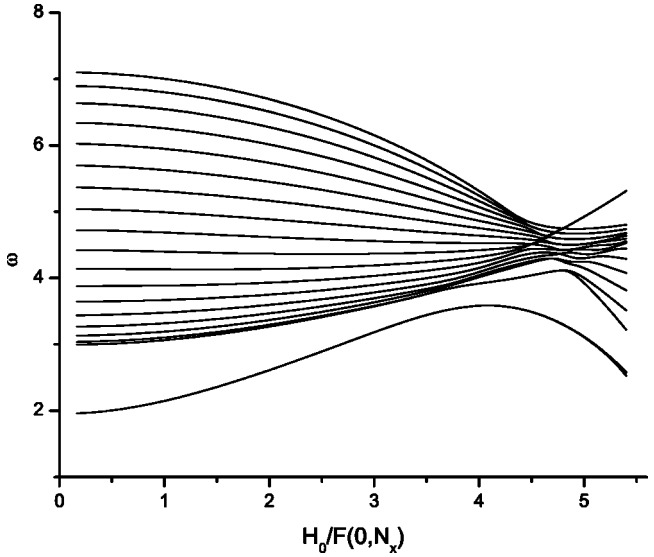

FIG. 11. Eigenfrequencies of a low-field ground state with nonperiodic boundary conditions; $J=0$, 21 dipoles.

Other modes ("bulk" modes) are simply standing sine waves with circular (constant tipping angle) orbits, as presented in Fig. 6.

E. Modes of equilibrium states in the presence of a weak external field

For the case where the external field is insufficient to align all spins parallel to it, different configurations occur from those presumed in the above discussion. We discuss two cases: In one case the lowest energy state corresponds to all dipoles tipped at a constant angle in the plane defined by the external field and the line axis. [Fig. 6]. When no external field is present this is the only possible configuration—all dipoles are parallel to the line axis. We should mention that

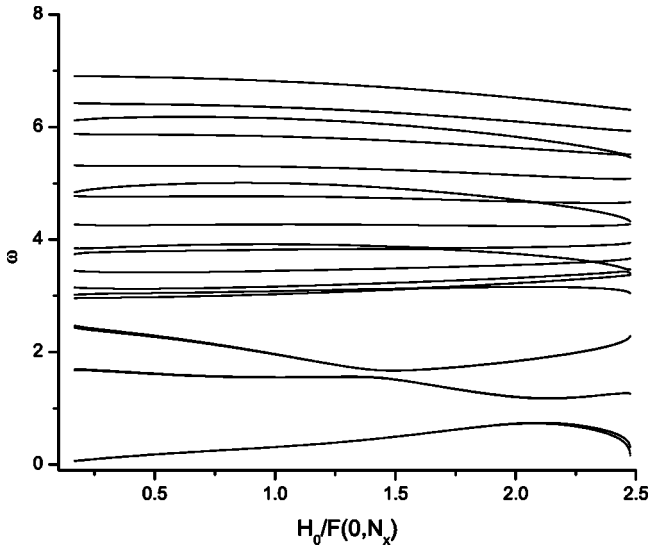

FIG. 12. Eigenfrequencies of a "2 kinks domain" state with periodic boundary conditions; $J=0$, 21 dipoles.

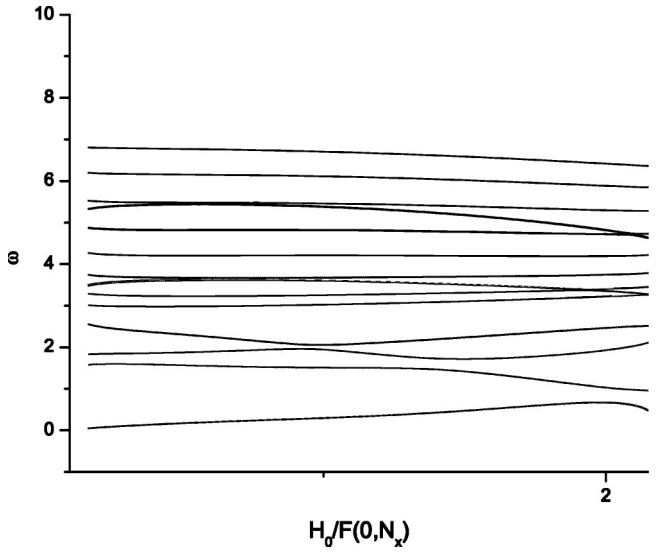

FIG. 13. Eigenfrequencies of a "2 kink domain" state with nonperiodic boundary conditions; $J=0$, 21 dipoles.

since all dipoles have the same direction, the exchange interaction plays no role.

Another possibility is what we can call "domain" states, shown in Fig. 7(b); as can be seen, one or more kink-like structures form, separating regions where groups of dipoles align anti-parallel to those in neighboring regions. This kind of configuration forms only in dipole-dipole, and not exchange, dominated samples. It is *metastable*, with the energy exceeding that of the ground state by approximately 11 energy units per kink. It does not exist if the applied field is either too strong or too weak to sustain it. More than one "domain" state (with different numbers of kinks) can form at the same time; however when periodic boundary conditions are applied, only configurations with an even number of kinks are possible.

We also mention that there are a number of unstable states for which the dipoles are oriented parallel to the local magnetic field and as a result experience no torque; but a small perturbation will force the system out of such configurations. It is noteworthy that these states have complex eigenvalues.

The ground state appears when the expression for the frequency given in Eq. (4.11) gives a complex result:

$$\frac{H_0}{M_s} < 6\sum_{d=1}^{N}\left(\frac{1}{d^3}\right),$$

$$\frac{H_0}{M_s} < 6F(0,N). \tag{4.13}$$

Requiring that dipoles should be parallel to the local magnetic field, we have

$$\sin\varphi = \frac{H_0}{6M_sF(0,N)}, \tag{4.14}$$

where φ is the angle between the dipoles and the x axis. The energy per dipole in this case is a constant:

$$\frac{E}{N} = -4M_sF(0,N). \tag{4.15}$$

The modes of such a system are given by

$$m_{ix}^{(1)} = ae^{ikx},$$

$$m_{iy}^{(1)} = ibe^{ikx}, \tag{4.16}$$

$$m_{iz}^{(1)} = -m_{ix}^{(1)}\sqrt{\frac{36M_s^2F^2(0,N)}{H_0^2}-1}.$$

Then

$$\omega^2 = \frac{\gamma^2M_s^2}{3}[F(k,N)+J(1-\cos(k))+2F(0,N)]\cdot\left[\left(12-\frac{H_0^2}{M_s^2F^2(0,N)}\right)F(k,N) - \frac{2}{3}J\left(\frac{H_0^2}{M_s^2F^2(0,N)}-18\right)\cos(k)+24F(0,N)+12J\right],$$

which is always positive if Eq. (4.13) is satisfied,

$$\frac{a^2}{b^2} = \frac{H_0^2}{3M_s^2F^2(0,N)}\frac{[F(k,N)+J(1-\cos(k))+2F(0,N)]}{\left(12-\frac{H_0^2}{M_s^2F^2(0,N)}\right)F(k,N)-\frac{2}{3}J\left(\frac{H_0^2}{M_s^2F^2(0,N)}-18\right)\cos(k)+24F(0,N)+12J}. \tag{4.17}$$

There is a double degeneracy due to the fact that frequency does not depend on the sign of the wave vector. For the case with only a dipole-dipole interaction the frequencies vs the applied magnetic field is shown in Fig. 8. There is one frequency which is independent of the applied magnetic field (in Fig. 8, $J=0$):

$$\omega = 2\gamma M_s[J+2F(0,N)]. \tag{4.18}$$

In Fig. 9 the dispersion dependence on the applied field is shown.

In Fig. 10 we show the eigenfrequencies vs the applied field for the case when, in addition to the dipole-dipole in-

teraction, we have an exchange interaction with $J=10$.

Figure 11 shows the eigenfrequencies vs the applied field for nonperiodic boundary conditions (obtained numerically).

The remaining case is what we have previously called a "domain" state. Figures 12 and 13 show the eigenfrequencies vs the applied field for the case of periodic and nonperiodic boundary conditions.

V. CONCLUSIONS

We have developed a method for finding the eigenfrequencies of an arbitrarily shaped body in the discrete dipole approximation. The effects of exchange and anisotropy energy are easily incorporated. In this first paper we have applied the method to find analytic solutions for two simple cases of a line of spins obeying periodic boundary conditions which are dipole analogous of the well known Bloch spin wave. The case of nonperiodic boundary conditions, for which the eigenvalues were obtained numerically, was also discussed.

Calculations on disks and spheres have been carried out, which will be discussed in subsequent papers. Modes associated with higher-dimensional objects will be discussed in subsequent papers, as well as using this method to describe the absorption properties and scaling approach, which allows one to describe relatively large systems using far less spins than the actual number of spins forming such systems.

We would like to thank A. Garg and V. Chandrasekhar for discussions. This work was supported by the National Science Foundation under Grant No. ECS-0224210.

[1] H. Suhl, Phys. Rev. **101**, 1437 (1956); Proc. IRE **44**, 1270 (1956); Phys. Chem. Solids **1**, 209 (1957); J. Appl. Phys. **29**, 416 (1958).
[2] J. Mercereau and R. P. Feynman, Phys. Rev. **104**, 63 (1956).
[3] L. R. Walker, Phys. Rev. **105**, 390 (1957).
[4] For a review see: L. R. Walker, *Spin Waves and Other Magnetic Modes, in Magnetism*, edited by G. T. Rado and H. Suhl (Academic Press, New York, 1963), Vol. 1.
[5] P. C. Fletcher and R. O. Bell, J. Appl. Phys. **30**, 687 (1959).
[6] P. C. Fletcher, I. H. Solt, Jr., and R. Bell, Phys. Rev. **114**, 739 (1959).
[7] R. Plumier, Physica (Amsterdam) **28**, 423 (1962).
[8] J. R. Eshbach and R. W. Damon, Phys. Rev. **118**, 1208 (1960).
[9] P. Politi, M. G. Pini, and A. Rettori, Phys. Rev. B **46**, 8312 (1992).
[10] J.-P. Nguenang, A. J. Kenfack, and T. C. Kofane, *Dipolar Effects on Soliton Dynamics on a Discrete Ferromagnetic Chain*, The Abdus Salam International Centre for Theoretical Physics.
[11] J. d'Albuquerque e Castro, D. Altbir, J. C. Retamal, and P. Vargas, Phys. Rev. Lett. **88**, 237202 (2002).
[12] For a discussion of the gradient energy see E. M. Lifshitz and L. P. Pitaevskii, *Statistical Physics* (Pergamon Press, New York, 1980), Part II, Sec. 69.
[13] A code developed by the U.S. National Institute for Standards and Technology is available for this purpose.
[14] S. Jung, J. B. Ketterson, and V. Chandrasekhar, Phys. Rev. B **66**, 132405 (2002).